Original Article

Pattern of Dopamine Transporter Density, Glucose Metabolism, and Amyloid Deposition in Patients with Alpha-Synucleinopathies and Alzheimer's Disease

Attapon Jantarato BSc[1], Anchisa Kunawudhi MD[1], Chetsadaporn Promteangtrong MD[1], Chanisa Chotipanich MD[1]

[1] National Cyclotron and PET Centre, Chulabhorn Hospital, Chulabhorn Royal Academy, Bangkok, Thailand

Background: The group of diseases including dementia with Lewy bodies (DLB), Parkinson's disease (PD), and Parkinson's disease dementia (PDD) are related to synucleinopathies. In addition to Alzheimer's disease (AD), these are common neurodegenerative diseases that share clinical features leading to difficulties in diagnosis. Hence, molecular imaging showing correlation with pathogenesis is recognized as a critical tool for improving the efficiency of differential diagnosis.

Objective: To determine characteristic patterns of dopamine transporter (DAT) density using ^{99m}Tc-TRODAT-1 (TRODAT-1), glucose metabolism using ^{18}F-fludeoxyglucose (FDG) and amyloid deposition using ^{11}C-Pittsburgh compound B (PiB) among these diseases.

Materials and Methods: Twenty-five individuals participated in the present study and included four healthy controls (HC), eight DLB, two PD, six PDD, and five AD. All subjects underwent FDG and PiB positron emission tomography (PET) and TRODAT-1 single-photon emission computed tomography (SPECT), with visual and semi-quantitative analysis of imaging.

Results: All subjects for synucleinopathy groups (DLB, PD, and PDD) had positive TRODAT-1 SPECT scintigraphy, while the AD and HC groups showed negative results. The positive PiB PET results were 100% in the AD, 33.33% with two of six cases in the PDD group, 37.5% with three of eight cases in the DLB group, and 0% in both the HC and PD groups. The hypometabolism patterns in PDD and AD groups were noted at parietotemporal region and parietotemporal, posterior cingulate, and precuneus regions, respectively. Meanwhile, the DLB hypometabolism pattern was found at parietotemporal, posterior cingulate, precuneus regions, and occipital lobe regions. None of the subjects in the HC or PD groups showed hypometabolism.

Conclusion: Positive TRODAT-1 SPECT provided an informative pattern for differential diagnosis among alpha-synuclein-related diseases, AD, and HC. Remarkably, hypometabolism in the occipital region can be used to differentiate DLB from AD, PDD, and PD. The amyloid deposition pattern in DLB and PDD groups was not significantly different.

Keywords: alpha-synucleinopathies; PET; SPECT; ^{99m}Tc-TRODAT-1; Alzheimer's disease

Received 24 May 2021 | Revised 30 July 2021 | Accepted 30 July 2021

J Med Assoc Thai 2021;104(11):1788-800

Website: http://www.jmatonline.com

Alzheimer's disease (AD), dementia with Lewy bodies (DLB), Parkinson's disease (PD), and Parkinson's disease dementia (PDD) are common types of dementia that require specific disease management[1,2]. However, difficulties in differential diagnosis among these diseases are of concern because of similarities in clinical, neurophysiological, and pathological features. Standard diagnoses for these conditions depend on clinical symptom presentation, which may require time for an accurate and precise diagnosis[3].

In the past decade, positron emission tomography (PET) or single-photon emission computed tomography (SPECT) imaging have emerged as tools with high potential for examining brain function in the living body. They have been used in combination with clinical information to improve disease diagnosis[4-7]. Although AD, DLB, PDD, or PD share clinical features, distinct patterns can be described at the molecular level. Amyloid plaque retention in AD presents as one such hallmark. Hence, molecular imaging of amyloid accumulation in the brain with amyloid-specific agents such as ^{11}C-Pittsburgh compound B (PiB) represent a highly precise way for early detection of AD in suspected

Correspondence to:

Jantarato A.

National Cyclotron and PET Centre, Chulabhorn Hospital, Chulabhorn Royal Academy, 906 Kamphaeng Phet 6 Road, Talat Bang Khen, Lak Si, Bangkok 10210, Thailand.

Phone: +66-2-5743355 ext. 1211

Email: attapon.jan@pccms.ac.th

How to cite this article:

Jantarato A, Kunawudhi A, Promteangtrong C, Chotipanich C. Pattern of Dopamine Transporter Density, Glucose Metabolism, and Amyloid Deposition in Patients with Alpha-Synucleinopathies and Alzheimer's Disease. J Med Assoc Thai 2021;104:1788-800.

doi.org/10.35755/jmedassocthai.2021.11.12949

patients[8-11]. In contrast, the group of parkinsonian disorders including DLB and PD/PDD are linked to synucleinopathy. The α-synuclein is a protein thought to play a role in maintaining a supply of synaptic vesicles in presynaptic terminals. The protein has also been suggested to be involved in regulating the release of the neurotransmitter dopamine in controlling voluntary and involuntary movements, which cannot be directly examined in vivo. Functional imaging agents such as TRODAT-1 play an important role in this type of disease because of specific binding to the dopamine active transporter (DAT), which is a key protein in regulating the dopaminergic system. DAT imaging enables assessment of dopamine terminal innervation at the striatum[10,12-15].

In addition, interestingly, although independent examination of dopaminergic and amyloid imaging may provide information for differential disease diagnosis, intersections between characteristic imaging patterns for AD, DLB, and PD/PDD may still be discovered because of imperceptible pathophysiology and disease progression[10]. Therefore, a combination of radiotracers and metabolic patterns using ^{18}F-fludeoxyglucose (FDG) may enhance the accuracy and precision of diagnosis[16]. Consequently, in the present study, the authors aimed to examine characteristic patterns of glucose metabolism using ^{18}F-FDG, amyloid deposition using ^{11}C-PiB, and dopamine transporter density using ^{99m}Tc-TRODAT-1 in patients with DLB, PD, PDD, and AD.

Materials and Methods

The present study was approved by the Human Research Ethics Committee of Chulabhorn Research Institute (EC number 024/2559, 061/2560). Written informed consents were obtained from all participants before the study.

Participants

Twenty-five participants, consisting of four healthy controls (HC) including two males and two females aged 41 to 83 years (mean age ± standard deviation [SD]: 62.25±17.15 years), eight DLB including four males and four females aged 60 to 80 years (mean age±SD: 72.63±8.03 years), two PD including one male and one female aged 74 and 75 years (mean age±SD: 74.5±0.5 years), six PDD including five males and one female aged 70 to 81 years (mean age±SD: 75.83±4.26 years), and five AD including two males and three females aged 63 to 95 years (mean age±SD: 80.2±11.38 years), enrolled in the present prospective study between August 2016 and July 2020.

No HC had a history of psychological or neurological disease, psychotropic drug use, or cancer within the last five years, with examinations from neurologists and neuropsychiatrists, participated in the study. They also had a score of more than 25 on the Montreal Cognitive Assessment Thai version. Participants with AD, DLB, PD, and PDD were assessed and diagnosed by the clinicians using the National Institute on Aging-Alzheimer's Association criteria for probable AD[17], Clinical Diagnostic Criteria for Parkinson's disease (MDS-PD criteria)[18] for PD, PDD and criteria for the clinical diagnosis of probable and possible DLB according to consensus report of the DLB Consortium for DLB clinical diagnosis[19].

Procedures

All participants underwent amyloid PET with ^{11}C-PiB and glucose metabolism with ^{18}F-FDG, using a Siemens Biograph 16 scanner (Siemens Healthcare GmbH, Erlagen, Germany) in three-dimensional (3D) mode. The TRODAT-1 SPECT was performed by using a SPECT/CT GE Discovery NM 670 (GE Healthcare, Chicago, Illinois, United States). For each patient, the three scans were performed within two weeks. Magnetic resonance imaging (MRI) was performed in all participants.

^{11}C-PiB imaging: All participants were scanned using a Siemens Biograph 16 scanner in 3D mode. Dynamic imaging was performed immediately after intravenous injection of 555 MBq (15 mCi) of ^{11}C-PiB. Dynamic brain PET/computed tomography (CT) scanning was performed for 70 minutes. Brain CT images were also acquired for attenuation correction. Image acquisition used a matrix size of 168, zoom of 1, and Gaussian filter with a full-width at half-maximum (FWHM) of 5.0. Images were reconstructed into seven frames of 10 minutes per frame using ordered subset expectation maximization (OSEM) with four iterations, eight subsets, and 4 mm pixel size.

^{18}F-FDG imaging: All participants fasted for six hours before scanning using a Siemens Biograph 16 scanner in 3D mode. Imaging was then performed 50 minutes after intravenous injection of 5 MBq/kg ^{18}F-FDG. Levels of plasma glucose were determined prior to the ^{18}F-FDG PET/CT study. Plasma glucose levels of less than 140 mg/dL were considered as acceptable for all patients. Image acquisition was performed for 10 minutes per bed position, with matrix size=256×256, zoom=1, and Gaussian filter

of FWHM=2.0. Image reconstruction was performed using OSEM with four iterations and eight subsets.

^{99m}Tc-TRODAT-1 imaging: All participants were scanned using a SPECT/CT GE Discovery NM 670 (GE Healthcare, Chicago, Illinois, United States). Imaging was then performed four hours after intravenous injection of 814 MBq (22 mCi.) of ^{99m}Tc-TRODAT-1. Image acquisition was performed using SPECT CT/CT acquisition mode for 20 second per angle in a head-first supine position, with matrix size=128×128, zoom=1.14, total angular range=2×360, view angel=3, energy setting=140.5 keV, and window width=20%. Image reconstruction was performed using OSEM with six iterations and ten subsets. A Gaussian filter of FWHM was used with x, y pixels=2 and Z=4, correction option: scatter correction=off, attenuation correction method was Chang's order 0, threshold 5, and coefficient 0.11.

MRI acquisition

T1-weighted MRI was acquired in all participants with following parameters: 3.0-T Philips MRI system. The parameters for the 3D T1MRI included: voxel size 0.43/0.43/1.20 mm, no overlapping; TR of 6.4 ms; TE of 3.0 ms, which reconstructed to 512×512 over a field of view of 220×200 mm. for registration and delineation of brain reference regions using the PMOD Neuro Tool (PMOD Technologies, Zürich, Switzerland). In addition, structural MRI imaging was applied for accessing eligible clinical criteria for diagnosis DLB, PD/PDD, and AD group following these demonstrated characteristics.

AD: the cognitive impaired patients employing structural imaging represented the medial temporal lobe atrophy without white matter hyper intensity[20,21].

DLB: absent or mild medial temporal lobe atrophy with white matter hyper intensity and parietooccipital atrophy or diffuse atrophy[21-23].

PD: abnormalities of the substantia nigra, such as volume loss, decreased T2 signal reflecting iron deposition, and blurring of the margins or unspecific or unremarkable[23].

PDD: cortical atrophy and ventricular dilatation with white matter lesions[24].

Statistical analysis and data assessment

Data processing and analyses of PET images were performed using the PMOD Neuro Tool (PMOD Technologies, Switzerland). ^{11}C-PiB PET images were automatically co-registered within each individual. The PET images were then registered to the T1MRI from each subject. The T1-MRI images were used for the registration and delineation of the brain reference regions, with the data being standardized to the Montreal Neurological Institute (MNI) T1MRI template atlas. VOIs were automatically outlined on the normalized MRI based on the maximum probability following the automated anatomical labeling (AAL)-merged atlas. Then, the standardized uptake value ratios (SUVR) of ^{11}C-PiB were calculated for various brain regions, using the cerebellum as a reference region. The measured areas including prefrontal, orbitofrontal, precuneus, parietal, anterior cingulate, and posterior cingulate. In the final process, SUVR for all mentioned areas were sum and averaged into the global SUVR. The defined areas of interest were applied from the Centiloid atlas VOI[25].

Stata, version 13 (StataCorp LP, College Station, TX, USA) was applied for all analyses. Ranked base non-parametric ANOVA (Kruskal-Wallis H test) and post-hoc Tukey HSD test were performed to compare mean of global SUVR among all groups with p-values of less than 0.05 being indicated statistical significance. As well as, the conduct of Box and Whisker plot for individual's SUVR for all groups.

Visual assessment of PET imaging from ^{18}F-FDG, ^{11}C-PiB, and ^{99m}Tc-TRODAT-1 were separately verified by three experienced, five-years specially trained nuclear medicine physicians blinded to the clinical data. Any disagreement results among the three nuclear medicine physicians were discussed for consensus. The agreement results were considered by at least two nuclear medicine physicians. Multi-planar images were examined using Syngovia Dicom viewer software (Siemens Healthineers GmbH, Erlagen, Germany) and the Xeleris workstation (GE Healthcare, Chicago, Illinois, United States). Finally, post-PET results were verified again with the clinical diagnosis by clinicians.

Results

Twenty-five participants were enrolled in the present study. Participants' characteristics are shown in Table 1.

Visual assessment results of all patients in the five groups were correlated to clinical diagnoses. Imaging results of all participants are shown in Table 2. Examples of imaging cases in each group are illustrated in Figure 1-5.

^{18}F-FDG

Glucose metabolism in the HC and PD groups was unremarkable in all patients. There was

Table 1. Participant' s characteristics

	Subjects				
	HC	AD	DLB	PD	PDD
Number	4	5	8	2	6
Age (years); mean±SD (range)	62.25±17.15 (41 to 83)	80.2±11.38 (63 to 95)	72.63±8.03 (60 to 80)	74.5±0.5 (74 to 75)	75.5±3.6 (70 to 81)
Sex; n (%)					
Male	2 (50)	2 (40)	4 (50)	1 (50)	5 (83)
Female	2 (50)	3 (60)	4 (50)	1 (50)	1 (1.7)

HC=healthy controls; AD=Alzheimer's disease; DLB=dementia with Lewy bodies; PD=Parkinson's disease; PDD=Parkinson's disease dementia; SD=standard deviation

Table 2. Imaging results of all participants

Group	Sex	Age (years)	Hypometabolism area of ^{18}F-FDG	^{99m}Tc-TRODAT-1	Increasing uptake area of ^{11}C-PiB	SUVR
HC	F	41	• Negative	• Negative	• Negative	1.09
	F	62	• Negative	• Negative	• Negative	0.58
	M	63	• Negative	• Negative	• Negative	0.57
	M	83	• Negative	• Negative	• Negative	0.63
AD	F	82	• Bilateral fronto-parietotemporal • Precuneus • Posterior cingulate gyrus	• Negative	• Posterior frontal • Parietal • Bilateral temporal lobes	1.57
	F	62	• Bilateral fronto-parietotemporal lobes	• Negative	• Throughout cortical regions	1.16
	M	63	• Bilateral parietotemporal lobes • Precuneus • Posterior cingulate gyrus	• Negative	• Bilateral cortical regions	1.93
	M	83	• Bilateral parietotemporal lobes • Precuneus • Posterior cingulate gyrus	• Negative	• Throughout cortical regions	2.52
	F	95	• Bilateral fronto-parietotemporal lobes • Precuneus • Posterior cingulate gyrus	• Negative	• Mild focal increased uptake at - Frontal - Parietal - Bilateral temporal lobes	1.5
DLB	M	66	• Bilateral parietal-temporal-occipital lobes • Cingulate island sign	• Bilateral caudate and putamen	• Negative	1.14
	F	67	• Hypometabolism in bilateral parietal-temporal-occipital lobes; more severe on the right occipital lobe	• Bilateral putamen	• Negative	1.17
	F	80	• Bilateral parietal-temporal-occipital lobes • Precuneus • Posterior cingulate gyrus; more severe on the left side	• Severely decreased uptake at the left putamen. • Mildly decreased uptake at both caudate and the right putamen	• Throughout cortical regions	1.49
	M	69	• Entire cerebral cortex; more prominent at the right frontal • Right parietotemporal regions • Precuneus • Posterior cingulate gyrus • Occipital lobe	• Markedly decreased uptake at bilateral caudate and putamen regions	• Negative	1.08
	M	80	• Bilateral posterior cingulate cortex • Bilateral parietotemporal • Bilateral occipital lobes	• Bilateral caudate and putamen regions	• Negative	1.1

M=male; F=female; FDG=fluorodeoxyglucose; TRODAT-1=dopamine active transporter tracer; PiB=Pittsburgh compound B; HC=healthy control; AD=Alzheimer's disease; DLB=Dementia with Lewy bodies; PD=Parkinson's disease; PDD=Parkinson's disease dementia

Table 2. (continued)

Group	Sex	Age (years)	Hypometabolism area of ^{18}F-FDG	^{99m}Tc-TRODAT-1	Increasing uptake area of ^{11}C-PiB	SUVR
DLB	M	80	• Markedly decreased uptake at bilateral anterior frontal • Bilateral parietal • Bilateral temporal lobes • Bilateral occipital lobes	• Markedly decreased uptake at bilateral putamen regions • Mildly decreased uptake at bilateral caudate regions	• Bilateral frontal cortices • Bilateral parietal • Bilateral temporal • Bilateral occipital lobes	1.7
	F	60	• Bilateral precuneus • Posterior cingulate gyrus • Parietotemporal • Bilateral occipital lobe	• Bilateral caudate and putamen regions; more prominent posteriorly	• Throughout cortical regions	2.17
	F	79	• Global reduction in cortical uptake; more prominent at cerebellum, • Posterior frontal • High parietal • Anterior temporal cortices • Bilateral occipital lobe	• Severely decreased uptake at bilateral caudate and putamen regions	• Negative	1.2
PD	F	74	• Negative	• Bilateral decrease uptake at putamen regions	• Negative	1.14
	M	75	• Negative	• Decreased uptake at bilateral caudate and putamen regions	• Negative	1.17
PDD	M	74	• Bilateral lateral parietal • Temporal lobes • Occipital sparing	• Bilateral putamen; more prominent on the right side	• Cortical uptake; more prominent on the frontal region • Parietal • Posterior cingulate regions	1.9
	M	73	• Bilateral precuneus • Parietotemporal lobes	• Bilateral caudate and putamen regions	• Negative	1.22
	M	81	• Bilateral parietotemporal lobes. • Slight decrease in uptake in the precuneus • Posterior cingulate cortex	• Decreased uptake at the right putamen	• Negative	0.97
	M	77	• Bilateral precuneus • Parietal • Bilateral temporal lobes • Occipital sparing	• Bilateral putamen regions	• Negative	1.4
	M	80	• Bilateral lateral parietal • Bilateral temporal lobesOccipital sparing	• Bilateral putamen with more prominent on the right side	• Cortex; more prominent on the frontal region • Parietal • Posterior cingulate	2.11
	F	70	• Left fronto-parietotemporal lobes • Occipital sparing	• Bilateral striatal regions	• Negative	0.99

M=male; F=female; FDG=fluorodeoxyglucose; TRODAT-1=dopamine active transporter tracer; PiB=Pittsburgh compound B; HC=healthy control; AD=Alzheimer's disease; DLB=Dementia with Lewy bodies; PD=Parkinson's disease; PDD=Parkinson's disease dementia

hypometabolism in bilateral fronto-parietotemporal regions, including the precuneus and posterior cingulate gyrus, but with occipital sparing in all patients of the AD group. Likewise, all subjects in the DLB and PDD groups demonstrated hypometabolism, except the hypometabolism in the DLB group occurred within the occipital lobe.

^{11}C-PiB

Amyloid retention throughout cortical regions was negative in the PD and HC groups, albeit with off-target binding in the white matter. There was abnormal uptake of PiB in the gray matter of all patients in the AD group, two positives in the PDD group, and three positives in the DLB group.

The range and mean SUVR ±SD of amyloid deposition is demonstrated in Table 3 and Figure 6. The highest was indicated in AD group, followed by PDD, DLB, and IPD group, and the lowest was in the HC group. The statistically significant difference

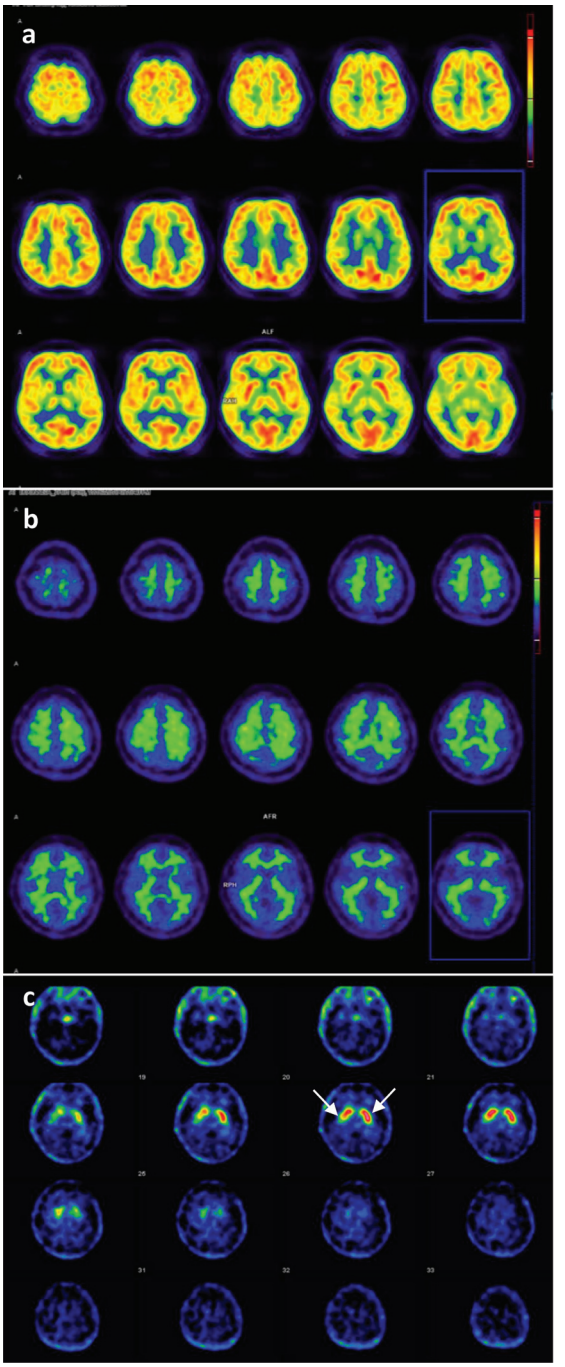

Figure 1. Axial Images of a 41-year-old female in HC group represented negative results in all radio-tracers study. (a) ^{18}F-FDG, (b) ^{11}C-PiB, (c) ^{99m}Tc-TRODAT-1 (long arrow).

between the five groups were accessed by Kruskal-Wallis test with p=0.023. However, there was only a significant pair test post hoc in HC and AD group (p=0.01) while the remaining pare-wise test were insignificant.

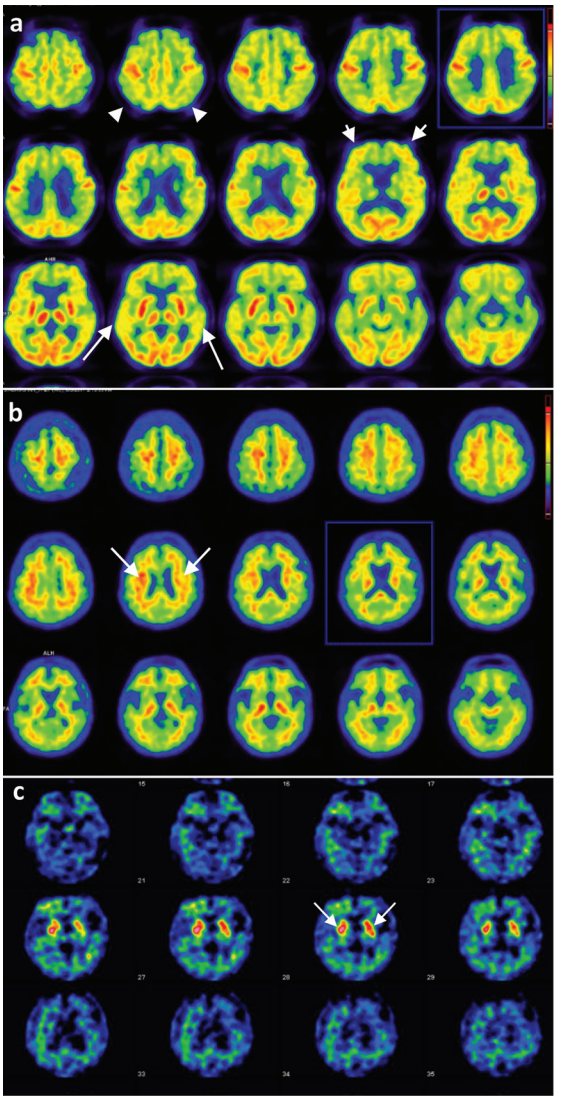

Figure 2. Axial images of an 81-year-old female in AD group. (a) ^{18}F-FDG PET imaging showed hypometabolism at the frontal (short arrow), temporal (long arrow), parietal (arrow head) regions, (b) ^{11}C-PiB image revealed global increased uptake at cortical cortex (long arrow), (c) ^{99m}Tc-TRODAT-1 showed the negative study (long arrow).

^{99m}Tc-TRODAT-1

Accumulation of TRODAT-1 in the striatum showed a normal uptake in the AD and HC groups. In contrast, dopamine deficiency was present in the caudate and putamen in all individuals of the DLB, PD, and PDD groups.

Discussion

Differential diagnosis of the various subtypes of dementia on clinical presentation is based on neurological tests and observation and evaluation

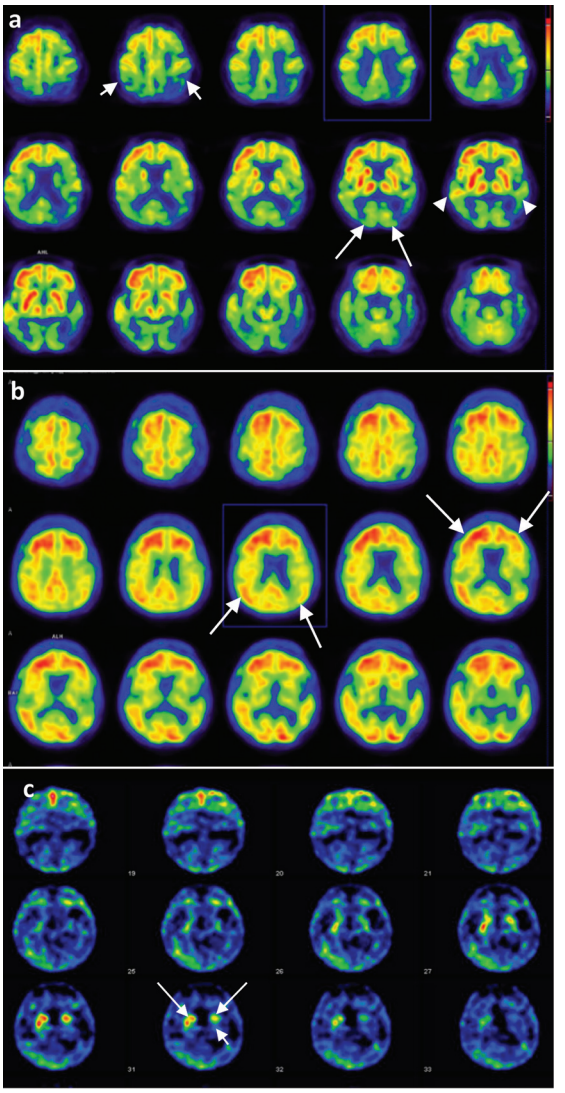

Figure 3. Axial Images of A 80-year-old female patient in DLB group. (a) ^{18}F-FDG image showed decreased uptake at bilateral parieto (short arrow), temporo (arrow head), occipital (long arrow) regions, (b) ^{11}C-PiB image represented increased amyloid deposition at the brain cortical regions (long arrow), (c) ^{99m}Tc-TRODAT-1 image showed markedly decreased uptake at left putamen and mild decreased uptake at both caudate (long arrow) and right putamen regions (short arrow).

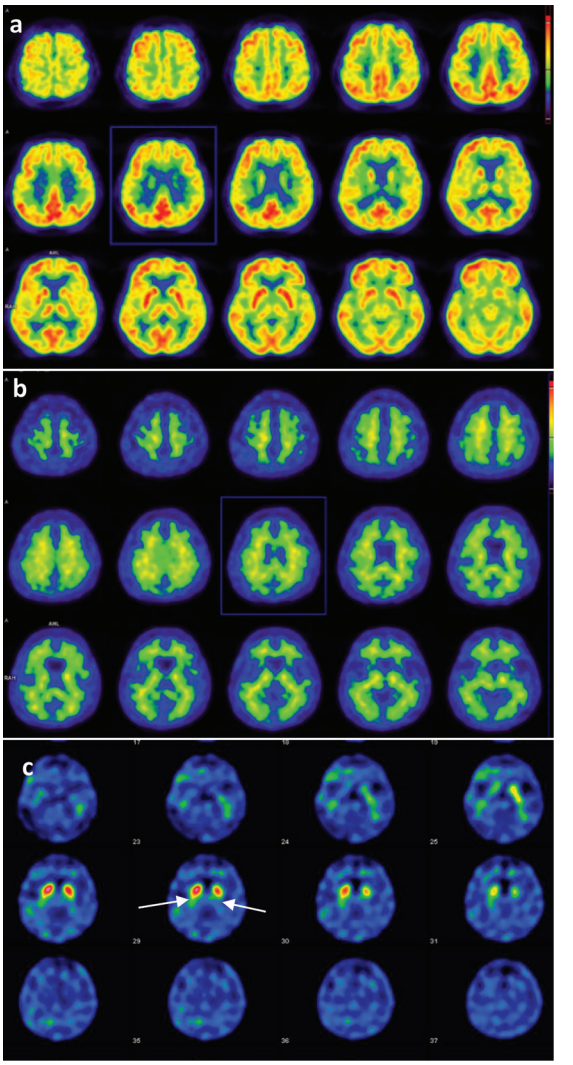

Figure 4. Axial images of A 74-year-old female patient in PD group. (a) a negative ^{18}F-FDG study, (b) a negative ^{11}C-PiB study, (c) ^{99m}Tc-TRODAT-1 image showed decreased uptake at bilateral putamen regions (long arrow).

by experienced psychiatrists or neurologists. Often, the diagnostic process is complicated and time consuming because of similarity or overlapping of clinical characteristics of related diseases. Hence, PET/SPECT examination with various radiotracers is used to aid diagnosis of a condition to increase both the specificity and accuracy of the diagnosis[26]. From the present study multi-tracer PET/SPECT study, negative results for all radiotracers were found in the HC group. Positive reports of AD, PD, and PDD were described by abnormal deposition of amyloid plaques, alteration of glucose metabolism, and striatal dopamine deficiency. These features could be related to clinical features and are distinctive when comparing between the different group of subjects.

Using FDG, the hypometabolism pattern in the AD group was found in the fronto-temporoparietal regions, which is in accordance with a previous study of patients with early AD. Areas of glucose hypometabolism are commonly observed in the parietotemporal association cortices, posterior cingulate cortex, and precuneus. With disease

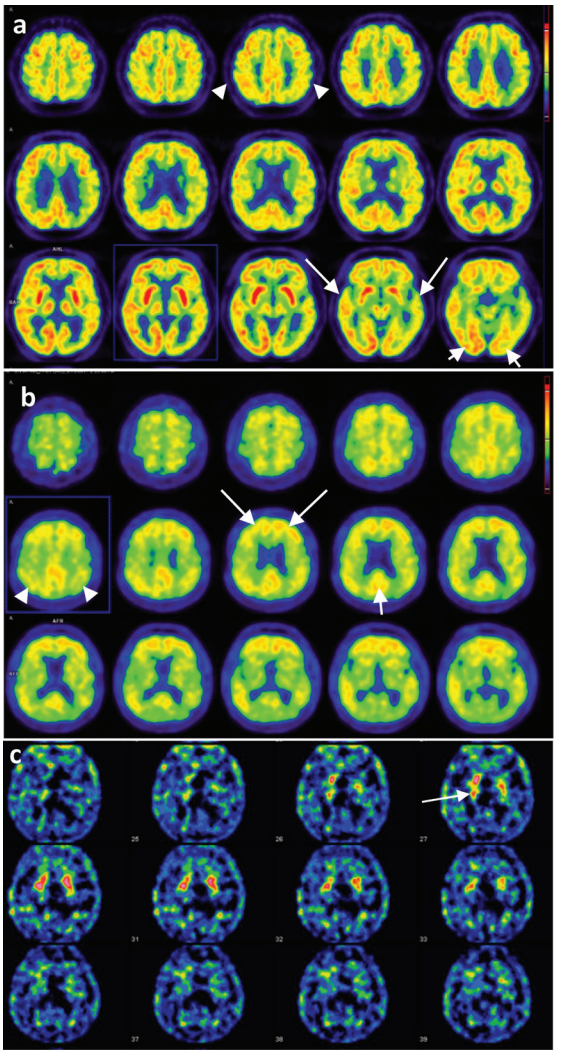

Figure 5. Axial images of A 80-year-old male patient in PDD group. a) ^{18}F-FDG showed decreased uptake at bilateral lateral parietal (arrow head), and bilateral temporal lobes (long arrow) with occipital sparing, (short arrow); b) ^{11}C-PiB image represented diffuse increased uptake in cortex with more prominent at frontal (long arrow), parietal (arrow head), and posterior cingulate regions (short arrow); c) ^{99m}Tc-TRODAT-1 image revealed decreased uptake at bilateral putamen with more prominent on the right side (long arrow).

progression, the regions involved spreads to the frontal cortices, whereas, metabolism in the striatum, thalamus, primary sensorimotor cortices, visual cortices, and cerebellum are relatively preserved[20,27,28].

In addition, the distinctive feature of amyloid as a neuropathological hallmark of AD can be demonstrated by abnormal amyloid deposition[29-31]. The amyloid load detected in all the AD subjects could be related to the neurological examination and pattern of hypometabolism in the patients.

Table 3. The mean, range and SD value of SUVR analysis with ^{11}C-PiB imaging

Group	n	Mean±SD	Range
HC	4	0.72±0.25	0.57 to 1.09
AD	5	1.74±0.52	1.16 to 2.52
DLB	8	1.38±0.39	1.08 to 2.17
IPD	2	1.12±0.04	1.14 to 1.17
PDD	6	1.43±0.48	0.97 to 2.11

HC=healthy control; AD=Alzheimer's disease; DLB=dementia with Lewy bodies; IPD=iPD=idiopathic Parkinson's disease; PDD=Parkinson's disease dementia; SD=standard deviation

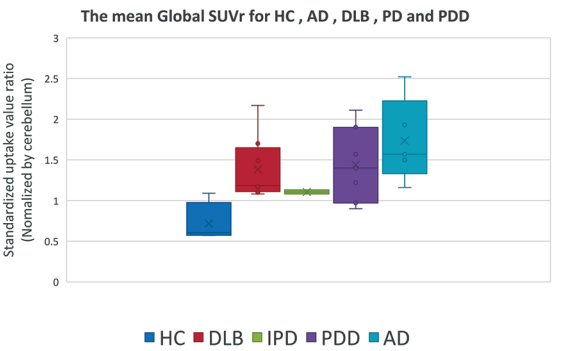

Figure 6. The Box and Whisker Plot of SUVR for each participant between HC, AD, DLB, PD and PDD groups.

Consistently, studies by Mosconi et al[32] and Furst et al[33] demonstrated amyloid deposition and hypometabolism in a similar pattern as detected in the present study. Moreover, a negative report of TRODAT-1 reflecting presynaptic dopaminergic signaling, is in accordance with a previous study by Piggott et al who noted that there was no change in the uptake site of dopamine in an AD group compared with normal controls[34].

Interestingly, a marked difference could be identified between alpha-synucleinopathy groups, including DLB, PD, and PDD. Abnormal dopamine transporters in the presynaptic region was shown in all subjects in this group and was the characteristic imaging pattern for differential diagnosis from AD[24]. Abnormal function of the dopaminergic system was related to accumulation of alpha-synuclein, which is a soluble endogenous protein. This protein shows preferential localization in presynaptic nerve terminals and interacts with vesicular phospholipids and proteins, suggesting a regulatory function in dopamine production, synaptic activity, and lipid vesicle trafficking. This specific protein normally regulates in the neuron cell, but when it comes to

the abnormality of protein regulation, it becomes aberrant protein soluble called protofibrils involving adverse effects to neuron cell such as disruption of cellular homeostasis and neuronal death, via effects on varieties intracellular targets and then contributes "synucleinopathy". The term "synucleinopathy" refers to a group of diverse neurodegenerative disorders including Parkinsonism, autonomic dysfunction, and non-motor deficits[35,36]. Hence, the effect of this protein to the dopaminergic system in brain is leading to reduction of DAT at striatal regions upon visualization by TRODAT-1 examination. Dopamine is a crucial neurotransmitter particularly for motor skills. Consequently, movement disorders or parkinsonian symptoms are often diagnosed among several types of dementias. Apart from that, DAT scan also has been considered as the effective tool for detection of nigro-striatal dopaminergic neurodegeneration associated with Parkinsonian as well as high specificity. It can be used to differentiate between disorders of essential tremor or drug induced PS, which does not have nigro-striatal dopamine transporter loss, from PS as true PS will have DAT degeneration. Usefulness of this tracer improves the clinical management and patients' quality of life. However, DAT scan cannot be used for differentiated among different PS syndrome[37,38]. Similarly, an abnormal DAT pattern is also described in various studies, such as by Walker et al[1] who showed differential diagnosis between DLB and AD using a dopaminergic presynaptic ligand. They described that both patients with DLB and PD had significantly lower uptake of radioactivity than patients with AD and controls in the caudate nucleus and anterior and posterior putamen. Comparable results were described by Rossi et al[39] who performed SPECT using ^{123}I-FP-CIT and ECD in 30 patients with PDD and 30 patients with DLB. They showed that striatal uptake of DAT tracer was statistically significant lower in patients with PDD and DLB compared with control data ($p<0.0005$).

Noticeably, not only a positive DAT scan but also differing hypometabolism in every subject can be a useful marker for differential diagnosis between AD and DLB. The hypometabolism observed in the occipital lobe is a prominent feature of the DLB group, while the hypometabolism was preserved in certain regions in the AD group. A comparable finding was described by Okamura et al[40] using statistical parametric mapping. They demonstrated a widespread metabolic reduction in the DLB group, particularly at the visual association cortex, compared with the AD group. Reduction at the occipital cortex was also linked to visual hallucinations in the DLB group, which is one of the commonest features of DLB, present in 54% to 70% of the patients[41]. The alteration of glucose metabolism found in PDD was similar to AD, with mostly reductions found in the lateral parietal and bilateral temporal lobes with occipital sparing in all patients. This is in contrast with the study by Edison et al[42] who studied microglia, amyloid, and glucose metabolism in PD with and without dementia. They identified aspects of FDG glucose separately. Nine out of 11 patients with PDD showed a significant reduction in glucose metabolism in the parieto-occipital or posterior cingulate cortex. Moreover, the study by Walker et al[43] also found greater metabolic deficits in the parietal and frontal regions in PDD, but that metabolic patterns in patients with PDD and LBD were broadly similar. Based upon the present study findings, the pattern of glucose metabolism present in the occipital region can be used as an indicator for differential diagnosis between DLB from AD and PDD. Further, in combination with DAT scan, differential diagnosis can be made among AD, DLB, and PDD. However, regarding the previous studies, the reduced pattern of FDG uptake for advanced PDD, which may spread to the occipital area, still needs consideration[44]. Furthermore, normal glucose metabolism was a characteristic that could differentiate PD from the remaining alpha-synucleinopathies of PDD and DLB, as well as AD. Comparably, a study by Broski et al[23] stated that the PD group showed generally preserved putamen activity, but in some cases, a reduction may be observed at the parieto-occipital cortex. Hence, even though metabolic imaging may not provide a distinctive pattern for PD compared with HC, a characteristic pattern could still be useful for differential diagnosis among idiopathic PD and other parkinsonian syndromes[23].

Amyloid imaging may play an important role in the diagnosis of AD and relates to the disease pathogenesis. However, when considering amyloid deposition in the parkinsonian group, which is linked to alpha-synuclein, there is concern regarding its identification. Deposition of amyloid was examined by Broski et al[23] who found normal amyloid for PD, while positive amyloid retention was reported in most cases of DLB, which is comparable to the present study finding. In addition, the authors found amyloid deposition in the DLB and PDD groups had two positives in the PDD group and three positives in the DLB group. Based upon the study of Gomperts

et al[45], who demonstrated a higher cortical amyloid burden in a DLB group over the PDD group, which was comparable to the AD group. Consistently, an amyloid imaging study by Foster et al[46] showed a lower percentage of PiB binding in patients with PDD (27%) compared to patients with DLB (33%). Moreover, Petrou et al[47] also demonstrated higher amyloid deposition in DLB group (0.68; 95% CI 0.55 to 0.82) compared with a PDD group (0.34; 95% CI 0.13 to 0.56). In relation to visual assessment, SUVR as the semi-quantitative tool of amyloid deposition contributed useful additional data when interpreted together with visual analyses. The present study semi-quantification revealed significant high SUVR across cortical brain compared to HC in all subjects of AD group. The high SUVR of amyloid retention at cortical brain have been represented in the typical AD. While, the second highest mean SUVR represented in DLB, PDD showed no statistically significant difference due to small observed group and diversity of deposition pattern showing both positive and negative individuals. Besides, HC and PD showing lower mean SUVR correlated to the visual interpretation describing the negative finding in all individuals. Regarding the semi-quantification method, there might be some variations of age-dependent amyloid load among elderly participants in the AD group. Whereas, a few participants could affect comparison results of calculated SUVR between both groups.

In case of AD, abnormal deposited plaque has been considered an hallmark of AD or even linked to cortical atrophy of both PDD and DLB[48,49]. Apart from this obvious representation, it is interesting that the present study observed results could be related to the previous findings revealing the uncertain conclusion regarding amyloid study between DLB and PDD. Many studies of amyloid PET imaging have been conducted for PD, PDD, and DLB. There are some notices to be identified as the significant elevated neocortical amyloid deposition is similar to Alzheimer disease. The impressive higher cortical is more prevalent in DLB than PDD[50-55]. Besides, the loss of brain volume is often more severe in DLB than PDD[48,56-58]. The positive amyloid may be represented with the advanced stage of both DLB and PDD[11]. This could be explained the varieties of amyloid pattern found on both diseases. Oppositely, a minority of reports state that there are higher PIB binding in PDD compared to DLB[35,50,51]. This overlapping pattern reported among prior studies are comparable with the present study. Although the positive number in DLB group tend to be higher, the cohort might be insufficient to appropriately conclude that DLB group reparented more prevalence of amyloid deposition compared to PDD.

Consequently, the authors may propose that due to the questionable intersection of pathological features between the DLB and PDD, amyloid imaging still needs future study with a larger patient cohort to further demonstrate the distinctive characteristics pattern. Furthermore, the correlation between the degree of cognitive impairment and the regional amyloid deposition might be an appropriate parameter as additional data to evaluate between DLB and PDD is required when only amyloid imaging was available.

Limitation

The present study was limited by a small number of participants to detect the true difference. Despite this limitation, the present study findings showed the distinctive patterns when comparing between alpha-synucleinopathies, as well as typical AD and HC groups. Moreover, these results could improve the accuracy and precision of diagnosis, particularly, if using multi radiotracers imaging with combined psychological assessment and neurological examination in the patients with uncertain clinical presentations. However, the present study findings were still preliminary and further study is needed with a large sample size to confirm the results.

Conclusion

The use of ^{99m}Tc-TRODAT-1 was beneficial for representation of a distinctive pattern for differential diagnosis among alpha-synuclein-related diseases, typical AD, and HC. Moreover, reduction of glucose metabolism in the occipital region effectively differentiated DLB from AD, PDD, and PD. A negative report of amyloid and normal glucose metabolism was also identified in patients with PD. Distinctly, the amyloid deposition pattern for both DLB and PDD is not significantly different and less likely to be identified compared with AD. Imaging examination by SPECT and PET using a combination of multiple radiotracers provides an effective diagnostic tool among dementia subtypes.

What is already known on this topic?

The alpha-synuclein-related neurodegenerative disease, such as PDD, DLB, PD, and Alzheimer's disease, are similar in clinical, neurophysiological, and pathological features, which specifically require differential diagnosis for appropriate management. Molecular imaging such as PET and SPECT can

access the pathogenesis pathways in molecular level with non-invasive method, leading to a significant improvement of differential diagnosis efficiency in these diseases.

What this study adds?

The use of PET and SPECT with highly specific and particularly combines radiopharmaceuticals could access and reveals different characteristic patterns in many diseases. The most distinctive pattern is the differentiation between PDD, DLB, PD, and Alzheimer's diseases, described by abnormal ^{99m}Tc-TRODAT-1 scan. Additionally, it is proposed that the amyloid depositions by using ^{11}C-PiB could typically be detected in AD and less likely in DLB and PDD patients. Nonetheless, the hypometabolism of DLB is likely to be found in the occipital region.

Acknowledgement

The authors would particularly extend their special thanks to Associate Professor Vorapun Senanarong MD, Department of Medicine, Faculty of Medicine Siriraj Hospital, Mahidol University for supporting this study.

Conflicts of interest

The authors declare no conflict of interest.

References

1. Walker Z, Costa DC, Walker RW, Shaw K, Gacinovic S, Stevens T, et al. Differentiation of dementia with Lewy bodies from Alzheimer's disease using a dopaminergic presynaptic ligand. J Neurol Neurosurg Psychiatry 2002;73:134-40.
2. Qiu C, Kivipelto M, von Strauss E. Epidemiology of Alzheimer's disease: occurrence, determinants, and strategies toward intervention. Dialogues Clin Neurosci 2009;11:111-28.
3. Caproni S, Colosimo C. Diagnosis and differential diagnosis of parkinson disease. Clin Geriatr Med 2020;36:13-24.
4. Pavese N, Brooks DJ. Imaging neurodegeneration in Parkinson's disease. Biochim Biophys Acta 2009;1792:722-9.
5. Brooks DJ, Frey KA, Marek KL, Oakes D, Paty D, Prentice R, et al. Assessment of neuroimaging techniques as biomarkers of the progression of Parkinson's disease. Exp Neurol 2003;184 Suppl 1:S68-79.
6. Shen LH, Tseng YC, Liao MH, Fu YK. The role of molecular imaging in the diagnosis and management of neuropsychiatric disorders. J Biomed Biotechnol 2011;2011:439397.
7. Ribeiro MJ, Vidailhet M, Loc'h C, Dupel C, Nguyen JP, Ponchant M, et al. Dopaminergic function and dopamine transporter binding assessed with positron emission tomography in Parkinson disease. Arch Neurol 2002;59:580-6.
8. Ishii K, Willoch F, Minoshima S, Drzezga A, Ficaro EP, Cross DJ, et al. Statistical brain mapping of 18F-FDG PET in Alzheimer's disease: validation of anatomic standardization for atrophied brains. J Nucl Med 2001;42:548-57.
9. Harding AJ, Halliday GM. Cortical Lewy body pathology in the diagnosis of dementia. Acta Neuropathol 2001;102:355-63.
10. Saeed U, Lang AE, Masellis M. Neuroimaging advances in Parkinson's disease and atypical parkinsonian syndromes. Front Neurol 2020;11:572976.
11. Ye R, Touroutoglou A, Brickhouse M, Katz S, Growdon JH, Johnson KA, et al. Topography of cortical thinning in the Lewy body diseases. Neuroimage Clin 2020;26:102196.
12. Jellinger KA. Dementia with Lewy bodies and Parkinson's disease-dementia: current concepts and controversies. J Neural Transm (Vienna) 2018;125:615-50.
13. Huang WS, Lin SZ, Lin JC, Wey SP, Ting G, Liu RS. Evaluation of early-stage Parkinson's disease with 99mTc-TRODAT-1 imaging. J Nucl Med 2001;42:1303-8.
14. Weng YH, Yen TC, Chen MC, Kao PF, Tzen KY, Chen RS, et al. Sensitivity and specificity of 99mTc-TRODAT-1 SPECT imaging in differentiating patients with idiopathic Parkinson's disease from healthy subjects. J Nucl Med 2004;45:393-401.
15. Geng Y, Shi GH, Jiang Y, Xu LX, Hu XY, Shao YQ. Investigating the role of 99mTc-TRODAT-1 SPECT imaging in idiopathic Parkinson's disease. J Zhejiang Univ Sci B 2005;6:22-7.
16. Meyer PT, Frings L, Rücker G, Hellwig S. (18) F-FDG PET in parkinsonism: differential diagnosis and evaluation of cognitive impairment. J Nucl Med 2017;58:1888-98.
17. McKhann GM, Knopman DS, Chertkow H, Hyman BT, Jack CR, Jr., Kawas CH, et al. The diagnosis of dementia due to Alzheimer's disease: recommendations from the National Institute on Aging-Alzheimer's Association workgroups on diagnostic guidelines for Alzheimer's disease. Alzheimers Dement 2011;7:263-9.
18. Marsili L, Rizzo G, Colosimo C. Diagnostic criteria for Parkinson's disease: from James Parkinson to the concept of prodromal disease. Front Neurol [Internet] 2018 [cited 2021 Feb 21];9:156. Available from: https://www.frontiersin.org/articles/10.3389/fneur.2018.00156/full.
19. McKeith IG, Boeve BF, Dickson DW, Halliday G, Taylor JP, Weintraub D, et al. Diagnosis and management of dementia with Lewy bodies: Fourth consensus report of the DLB Consortium. Neurology 2017;89:88-100.

20. Johnson KA, Fox NC, Sperling RA, Klunk WE. Brain imaging in Alzheimer disease. Cold Spring Harb Perspect Med 2012;2:a006213.
21. Park M, Moon WJ. Structural MR imaging in the diagnosis of Alzheimer's disease and other neurodegenerative dementia: current imaging approach and future perspectives. Korean J Radiol 2016;17:827-45.
22. Berman SB, Miller-Patterson C. PD and DLB: Brain imaging in Parkinson's disease and dementia with Lewy bodies. Prog Mol Biol Transl Sci 2019;165:167-85.
23. Broski SM, Hunt CH, Johnson GB, Morreale RF, Lowe VJ, Peller PJ. Structural and functional imaging in parkinsonian syndromes. Radiographics 2014;34:1273-92.
24. Petrou M, Kotagal V, Bohnen NI. An update on brain imaging in parkinsonian dementia. Imaging Med 2012;4:201-13.
25. Klunk WE, Koeppe RA, Price JC, Benzinger TL, Devous MD, Sr., Jagust WJ, et al. The Centiloid Project: standardizing quantitative amyloid plaque estimation by PET. Alzheimers Dement 2015;11:1-15. e1-4.
26. Suppiah S, Didier MA, Vinjamuri S. The Who, When, Why, and How of PET amyloid imaging in management of Alzheimer's disease-review of literature and interesting images. Diagnostics (Basel) 2019;9:65.
27. Marcus C, Mena E, Subramaniam RM. Brain PET in the diagnosis of Alzheimer's disease. Clin Nucl Med 2014;39:e413-22; quiz e23-6.
28. Mosconi L. Brain glucose metabolism in the early and specific diagnosis of Alzheimer's disease. FDG-PET studies in MCI and AD. Eur J Nucl Med Mol Imaging 2005;32:486-510.
29. Serrano-Pozo A, Frosch MP, Masliah E, Hyman BT. Neuropathological alterations in Alzheimer disease. Cold Spring Harb Perspect Med 2011;1:a006189.
30. Thal DR, von Arnim C, Griffin WS, Yamaguchi H, Mrak RE, Attems J, et al. Pathology of clinical and preclinical Alzheimer's disease. Eur Arch Psychiatry Clin Neurosci 2013;263 Suppl 2:S137-45.
31. De-Paula VJ, Radanovic M, Diniz BS, Forlenza OV. Alzheimer's disease. Subcell Biochem 2012;65:329-52.
32. Mosconi L, McHugh PF. FDG- and amyloid-PET in Alzheimer's disease: is the whole greater than the sum of the parts? Q J Nucl Med Mol Imaging 2011;55:250-64.
33. Furst AJ, Lal RA. Amyloid-β and glucose metabolism in Alzheimer's disease. J Alzheimers Dis 2011;26 Suppl 3:105-16.
34. Piggott MA, Marshall EF, Thomas N, Lloyd S, Court JA, Jaros E, et al. Striatal dopaminergic markers in dementia with Lewy bodies, Alzheimer's and Parkinson's diseases: rostrocaudal distribution. Brain 1999;122(Pt 8):1449-68.
35. Levigoureux E, Bouillot C, Baron T, Zimmer L, Lancelot S. PET imaging of the influence of physiological and pathological α-synuclein on dopaminergic and serotonergic neurotransmission in mouse models. CNS Neurosci Ther 2019;25:57-68.
36. Stefanis L. α-synuclein in Parkinson's disease. Cold Spring Harb Perspect Med 2012;2:a009399.
37. Saeed U, Compagnone J, Aviv RI, Strafella AP, Black SE, Lang AE, et al. Imaging biomarkers in Parkinson's disease and Parkinsonian syndromes: current and emerging concepts. Transl Neurodegener 2017;6:8.
38. Seifert KD, Wiener JI. The impact of DaTscan on the diagnosis and management of movement disorders: A retrospective study. Am J Neurodegener Dis 2013;2:29-34.
39. Rossi C, Volterrani D, Nicoletti V, Manca G, Frosini D, Kiferle L, et al. "Parkinson-dementia" diseases: a comparison by double tracer SPECT studies. Parkinsonism Relat Disord 2009;15:762-6.
40. Okamura N, Arai H, Higuchi M, Tashiro M, Matsui T, Hu XS, et al. [18F]FDG-PET study in dementia with Lewy bodies and Alzheimer's disease. Prog Neuropsychopharmacol Biol Psychiatry 2001;25:447-56.
41. Heitz C, Noblet V, Cretin B, Philippi N, Kremer L, Stackfleth M, et al. Neural correlates of visual hallucinations in dementia with Lewy bodies. Alzheimers Res Ther 2015;7:6.
42. Edison P, Ahmed I, Fan Z, Hinz R, Gelosa G, Ray Chaudhuri K, et al. Microglia, amyloid, and glucose metabolism in Parkinson's disease with and without dementia. Neuropsychopharmacology 2013;38:938-49.
43. Walker Z, Gandolfo F, Orini S, Garibotto V, Agosta F, Arbizu J, et al. Clinical utility of FDG PET in Parkinson's disease and atypical parkinsonism associated with dementia. Eur J Nucl Med Mol Imaging 2018;45:1534-45.
44. Peppard RF, Martin WR, Carr GD, Grochowski E, Schulzer M, Guttman M, et al. Cerebral glucose metabolism in Parkinson's disease with and without dementia. Arch Neurol 1992;49:1262-8.
45. Gomperts SN, Rentz DM, Moran E, Becker JA, Locascio JJ, Klunk WE, et al. Imaging amyloid deposition in Lewy body diseases. Neurology 2008;71:903-10.
46. Foster ER, Campbell MC, Burack MA, Hartlein J, Flores HP, Cairns NJ, et al. Amyloid imaging of Lewy body-associated disorders. Mov Disord 2010;25:2516-23.
47. Petrou M, Dwamena BA, Foerster BR, MacEachern MP, Bohnen NI, Müller ML, et al. Amyloid deposition in Parkinson's disease and cognitive impairment: a systematic review. Mov Disord 2015;30:928-35.
48. Mak E, Donaghy PC, McKiernan E, Firbank MJ, Lloyd J, Petrides GS, et al. Beta amyloid deposition maps onto hippocampal and subiculum atrophy in dementia with Lewy bodies. Neurobiol Aging 2019;73:74-81.

49. Lee YG, Jeon S, Yoo HS, Chung SJ, Lee SK, Lee PH, et al. Amyloid-β-related and unrelated cortical thinning in dementia with Lewy bodies. Neurobiol Aging 2018;72:32-9.
50. Jokinen P, Scheinin N, Aalto S, Någren K, Savisto N, Parkkola R, et al. [(11)C]PIB-, [(18)F]FDG-PET and MRI imaging in patients with Parkinson's disease with and without dementia. Parkinsonism Relat Disord 2010;16:666-70.
51. Rowe CC, Ng S, Ackermann U, Gong SJ, Pike K, Savage G, et al. Imaging beta-amyloid burden in aging and dementia. Neurology 2007;68:1718-25.
52. Shimada H, Shinotoh H, Hirano S, Miyoshi M, Sato K, Tanaka N, et al. β-Amyloid in Lewy body disease is related to Alzheimer's disease-like atrophy. Mov Disord 2013;28:169-75.
53. Maetzler W, Liepelt I, Reimold M, Reischl G, Solbach C, Becker C, et al. Cortical PIB binding in Lewy body disease is associated with Alzheimer-like characteristics. Neurobiol Dis 2009;34:107-12.
54. Kantarci K, Lowe VJ, Boeve BF, Weigand SD, Senjem ML, Przybelski SA, et al. Multimodality imaging characteristics of dementia with Lewy bodies. Neurobiol Aging 2012;33:2091-105.
55. Burke JF, Albin RL, Koeppe RA, Giordani B, Kilbourn MR, Gilman S, et al. Assessment of mild dementia with amyloid and dopamine terminal positron emission tomography. Brain 2011;134:1647-57.
56. Beyer MK, Larsen JP, Aarsland D. Gray matter atrophy in Parkinson disease with dementia and dementia with Lewy bodies. Neurology 2007;69:747-54.
57. Burton EJ, McKeith IG, Burn DJ, Williams ED, O'Brien JT. Cerebral atrophy in Parkinson's disease with and without dementia: a comparison with Alzheimer's disease, dementia with Lewy bodies and controls. Brain 2004;127:791-800.
58. Lee JE, Park B, Song SK, Sohn YH, Park HJ, Lee PH. A comparison of gray and white matter density in patients with Parkinson's disease dementia and dementia with Lewy bodies using voxel-based morphometry. Mov Disord 2010;25:28-34.